

Scintillation index for two Gaussian laser beams with different wavelengths in weak atmospheric turbulence

Avner Peleg¹ and Jerome V. Moloney^{1,2}

¹*Arizona Center for Mathematical Sciences,*

University of Arizona, Tucson, Arizona 85721, USA and

²*College of Optical Sciences, University of Arizona, Tucson, Arizona 85721, USA**

Abstract

We study propagation of two lowest order Gaussian laser beams with different wavelengths in weak atmospheric turbulence. Using the Rytov approximation and assuming a slow detector we calculate the longitudinal and radial components of the scintillation index for a typical free space laser communication setup. We find the optimal configuration of the two laser beams with respect to the longitudinal scintillation index. We show that the value of the longitudinal scintillation for the optimal two-beam configuration is smaller by more than 50% compared with the value for a single lowest order Gaussian beam with the same total power. Furthermore, the radial scintillation for the optimal two-beam system is smaller by 35%-40% compared with the radial scintillation in the single beam case. Further insight into the reduction of intensity fluctuations is gained by analyzing the self- and cross-intensity contributions to the scintillation index.

INTRODUCTION

Propagation of light through atmospheric turbulence is the subject of a rich and very active field of research owing to the many applications in free space laser communications, remote sensing, imaging systems and targeting [1, 2, 3]. In these applications it is usually desirable to find ways to reduce the turbulence effects on the propagating optical beam. In recent years there has been a renewed interest in using partially coherent sources of light as a method for reducing the turbulence effects and improving the system performance. Many works concentrated on the case where the optical source is spatially partially coherent. First, the properties of the mutual coherence function of spatially partially coherent beams propagating in atmospheric turbulence were analyzed [4, 5, 6]. Later on it was shown that intensity fluctuations of spatially partially coherent Gaussian beams can decrease as the coherence of the sources decreases [7, 8]. Additional computational evidence for the smaller sensitivity of spatially partially coherent beams to turbulence was obtained by considering the distance dependence of the coherence radius of the beam [9, 10]. More recently it was shown theoretically [11] and experimentally [12] that the effective propagation distance measuring beam spreading in a turbulent medium relative to free-space spreading is larger for spatially partially coherent beams than for fully coherent ones. Other works demonstrated the improved performance obtained by using spatially partially coherent beams in terms of the normalized intensity distribution [13], the mean squared beam width [14, 15], power in the bucket and Strehl ratio [15], the scintillation index [16], the bit error rate (BER)[16, 17, 18] and the average signal to noise ratio (SNR)[16].

Generation of spatially partially coherent beams in various setups, e.g., by focusing a laser beam on a rotating random phase screen, is quite straightforward. However, it is not clear to what extent such setups would fit in actual applications where reliability and compactness of the optical source play an important role. Furthermore, even though a theoretical method for optimizing a spatially partially coherent source was outlined in Ref. [19], the problem of implementing the method for realistic systems remains far from being resolved. Consequently, one has to look for other methods for generating the partial coherence, which are potentially more reliable and easier to optimize and to control. One very promising possibility is to look for a temporally partially coherent input optical field generated by using multiple laser beams with different wavelengths. Indeed, in a typical situation in which the

response time of the detector is large compared with the inverse of the frequency difference between any pair of beams in the input field, rapidly oscillating contributions to the total intensity would average out. As a result, one can expect smaller values of high moments of the intensity compared with corresponding values in the single wavelength case. This would in turn result in smaller values for the scintillation index and BER and higher values for the SNR.

We emphasize that generation of a temporally partially coherent source of light consisting of multiple laser beams with different wavelengths can be realized in a convenient and efficient manner by using an array of vertical external cavity surface lasers (VECSELs). These devices have the advantage of generating high power, high brightness wavelength tunable TEM₀₀ beams (lowest order Gaussian beams)[20]. Individual VECSEL devices have been demonstrated with powers of 50 Watts running multi-mode [21] and up to 10 Watts, single TEM₀₀ mode and spectrally narrow (<0.1nm line width) [22]. Moreover, the semiconductor multiple quantum well active mirror of these devices should allow for multi-GHz modulation rates for data transmission.

Propagation of temporally partially coherent light in atmospheric turbulence was first studied by Fante [23, 24]. Considering a single infinite plane wave this author obtained approximate analytic expressions for the scintillation index of the planar wave in the weak [23] and strong [24] turbulence regimes. Later studies extended these results to the cases of a spatially incoherent source [25] and a source that is partially coherent in both space and time [26]. More recently, Kiasaleh studied the scintillation index for a multiwavelength infinite plane wave in weak atmospheric turbulence [27, 28]. This author showed that use of a multiwavelength plane wave leads to an increase in the achievable SNR as well as in the upper bound on the SNR imposed by increasing the aperture size. These previous studies focused on infinite planar waves or on spherical waves, whereas in reality, Gaussian laser beams with finite initial spot size and possibly non-zero phase front radius of curvature are employed. Since the dynamics of the optical field strongly depends on the initial spot size and phase front radius of curvature it is important to take these characteristics into account when calculating turbulence effects. Furthermore, the fact that the optical field of N Gaussian laser beams depends on $2N$ additional parameters allows for a greater flexibility in optimization and control of the input field against turbulence effects. Thus, the lower values for high moments of the intensity combined with the greater flexibility make the setup

based on multiple Gaussian beams with different wavelengths very advantageous and call for a detailed investigation of the optical field dynamics in this setup.

In this paper we take this important task and study propagation of two lowest order Gaussian laser beams with different wavelengths in weak atmospheric turbulence. Using the Rytov approximation and assuming a slow detector we calculate the longitudinal component of the scintillation index for both the Kolmogorov spectrum and the Von Kármán spectrum. For a typical setup of a free space laser communication system we show that the longitudinal scintillation exhibits a minimum as a function of the initial beam separation. We interpret this minimum as corresponding to the optimal configuration of the two-beam system, where optimization is with respect to the value of the longitudinal scintillation. Moreover, the longitudinal scintillation for the optimal two-beam configuration is smaller by more than 50% compared with the longitudinal scintillation for a single lowest order Gaussian beam with the same total power. The existence of the longitudinal scintillation minimum is found to be independent of the turbulence spectrum. Furthermore, we calculate the total scintillation index for the optimal two-beam configuration using the Von Kármán spectrum and find that the values of the total scintillation are smaller by 12%-64% compared with the corresponding values for a single Gaussian beam with the same total power. Further insight into this improvement is gained by decomposing the total scintillation into self- and cross-intensity contributions. Finally, we show that the radial scintillation for the optimal two-beam system is smaller by 35%-40% than the radial scintillation in the single beam case.

The rest of the paper is organized as follows. In Section 2 we present the method used to calculate the scintillation index as well as general expressions for the scintillation index of a system consisting of N Gaussian laser beams with different wavelengths. In section 3 we analyze in detail the total scintillation index as well as its longitudinal and radial components for a two-beam system considering a typical setup of a free space laser communication system. Section 4 is reserved for discussion. In Appendix A we derive in detail some relations appearing in Section 1.

CALCULATION OF THE SCINTILLATION INDEX

We consider propagation of N lowest order Gaussian laser beams with different wavelengths λ_j , where $j = 1, \dots, N$, in weak atmospheric turbulence. For simplicity and without

loss of generality we assume that the beams are linearly polarized and propagate along the z axis. We denote by \mathbf{d}_j the locations of the beam centers at the input plane $z = 0$. Thus, the magnitude of the total electric field E at $z = 0$ is given by

$$E(\mathbf{r}, 0, t) = \sum_{j=1}^N E_j(\mathbf{r}_j, 0, t) = \sum_{j=1}^N U_j(\mathbf{r}_j, 0) \exp[-i\omega_j t], \quad (1)$$

where

$$U_j(\mathbf{r}_j, 0) = A_{0j} \times \exp\left[-\left(\frac{1}{W_{0j}^2} + \frac{ik_j}{2F_{0j}}\right)|\mathbf{r} - \mathbf{d}_j|^2\right]. \quad (2)$$

In Eqs. (1) and (2) E_j is the electric field due to the j -th beam, \mathbf{r} is the radius vector in the xy plane, $\mathbf{r}_j \equiv \mathbf{r} - \mathbf{d}_j$, t is time, $k_j = 2\pi/\lambda_j$ are the wave numbers and $\omega_j = k_j c$ are the angular frequencies, where c is the speed of light. In addition, A_{0j} are the initial on-axis amplitudes, W_{0j} are the initial spot sizes and F_{0j} are the initial phase front radii of curvature.

We assume that the intensity of the optical field is small enough so that its evolution is governed by the linear wave equation. Therefore, the dynamics of the fields U_j is described by

$$\nabla^2 U_j + k_j^2 [1 + n_1(\mathbf{r}, z)]^2 U_j = 0, \quad (3)$$

where $n_1(\mathbf{r}, z)$ stands for the turbulence induced fluctuation in the refractive index coefficient. The total optical field after propagating a distance $z = L$ is

$$E(\mathbf{r}, L, t) = \sum_{j=1}^N E_j(\mathbf{r}_j, L, t) = \sum_{j=1}^N U_j(\mathbf{r}_j, L) \exp[-i\omega_j t]. \quad (4)$$

Assuming weak turbulence, $|n_1(\mathbf{r}, z)| \ll 1$, Eq. (3) can be approximated by

$$\nabla^2 U_j + k_j^2 [1 + 2n_1(\mathbf{r}, z)] U_j = 0. \quad (5)$$

To solve Eq. (5) we use the Rytov perturbation method and express U_j as

$$U_j(\mathbf{r}_j, L) = U_{0j}(\mathbf{r}_j, L) \exp[\psi_j(\mathbf{r}_j, L; k_j)], \quad (6)$$

where U_{0j} is the field of the j -th beam in free space (in the absence of turbulence) and ψ_j is a complex field describing the effects of turbulence on the j -th beam and calculated perturbatively up to the second order in $n_1(\mathbf{r}, z)$.

Following the approach derived in Refs. [3, 29] we define the beam parameters Θ_{0j} and Λ_{0j} , which characterize the unperturbed beams in terms of the initial phase front radii of curvature F_{0j} and spot sizes W_{0j} , respectively

$$\Theta_{0j} = 1 - \frac{L}{F_{0j}}, \quad \Lambda_{0j} = \frac{2L}{k_j W_{0j}^2}. \quad (7)$$

We also use the beam parameters Θ_j and Λ_j , characterizing the unperturbed beams in terms of the phase front radii of curvature F_j and spot sizes W_j at distance L

$$\Theta_j = 1 - \frac{L}{F_j} = \frac{\Theta_{0j}}{\Theta_{0j}^2 + \Lambda_{0j}^2}, \quad \Lambda_j = \frac{2L}{k_j W_j^2} = \frac{\Lambda_{0j}}{\Theta_{0j}^2 + \Lambda_{0j}^2}. \quad (8)$$

The time-dependent total intensity of the N -beam system is

$$I(\mathbf{r}, L, t) = \sum_{j=1}^N I_j(\mathbf{r}_j, L) + \sum_j^N \sum_{m \neq j}^N E_j(\mathbf{r}_j, L, t) E_m^*(\mathbf{r}_m, L, t), \quad (9)$$

where $I_j = |E_j|^2 = |U_j|^2$ is the intensity of the j -th beam. The intensity measured by the detector can be defined as the following time average

$$I_{det}(\mathbf{r}, L) \equiv \langle I(\mathbf{r}, L, t) \rangle_{det} \equiv \frac{1}{\tau} \int_0^\tau dt I(\mathbf{r}, L, t), \quad (10)$$

where τ is the response time of the detector and $\langle \dots \rangle_{det}$ denotes time average in the detector. Assuming a slow detector and different wavelengths, $\lambda_j \neq \lambda_m$ for $j \neq m$, we neglect the terms $U_j U_m^*$ $j \neq m$, which are rapidly oscillating with time. [See also Ref. [27], where a similar approximation was made for multiple planar laser beams]. Thus, the average of the total intensity of the field is given by

$$I_{det}(\mathbf{r}, L) \equiv \langle I(\mathbf{r}, L, t) \rangle_{det} \simeq \sum_{j=1}^N I_j(\mathbf{r}_j, L). \quad (11)$$

We are interested in calculating the total scintillation index σ_I^2 which is defined by

$$\sigma_I^2(\mathbf{r}, L) \equiv \frac{\langle I_{det}^2(\mathbf{r}, L) \rangle}{\langle I_{det}(\mathbf{r}, L) \rangle^2} - 1, \quad (12)$$

where $\langle \dots \rangle$ (without any subscript) stands for average over different realizations of turbulence disorder. Using Eqs. (11) and (12) we obtain

$$\sigma_I^2(\mathbf{r}, L) = \frac{\sum_{j=1}^N \langle I_j^2(\mathbf{r}_j, L) \rangle + 2 \sum_j^N \sum_{m > j}^N \langle I_j(\mathbf{r}_j, L) I_m(\mathbf{r}_m, L) \rangle}{\left(\sum_{j=1}^N \langle I_j(\mathbf{r}_j, L) \rangle \right)^2} - 1. \quad (13)$$

Following the usual convention we decompose σ_I^2 into a longitudinal (\mathbf{r} -independent) component

$$\sigma_{I,l}^2(L) \equiv \sigma_I^2(0, L) \quad (14)$$

and a radial component

$$\sigma_r^2(\mathbf{r}, L) \equiv \sigma_I^2(\mathbf{r}, L) - \sigma_{I,l}^2(L). \quad (15)$$

Within the framework of the Rytov approximation the average intensity of the j -th laser beam is given by [3]

$$\langle I_j(\mathbf{r}_j, L) \rangle = I_{0j}(\mathbf{r}_j, L) \exp [H_{1j}(r_j, L)], \quad (16)$$

where

$$I_{0j}(\mathbf{r}_j, L) = \frac{A_{0j}^2 W_{0j}^2}{W_j^2} \exp \left[-\frac{2r_j^2}{W_j^2} \right] \quad (17)$$

and

$$H_{1j}(r_j, L) = 4\pi^2 k_j^2 L \int_0^1 d\xi \int_0^\infty d\kappa \kappa \Phi_n(\kappa) \times \left[I_0(2\Lambda_j r_j \xi \kappa) \exp \left(-\frac{\Lambda_j L \kappa^2 \xi^2}{k_j} \right) - 1 \right]. \quad (18)$$

In Eq. (18) $\xi = 1 - z/L$, κ is the wave number, $\Phi_n(\kappa)$ is the power spectral density of the refractive index fluctuations and $I_0(x)$ is the modified Bessel function of the first kind and zero order, $I_0(x) = J_0(ix)$, where $J_0(x)$ is the Bessel function of first kind and zero order [30]. The average of the second moment $\langle I_j^2(\mathbf{r}_j, L) \rangle$ is given by [3]

$$\langle I_j^2(\mathbf{r}_j, L) \rangle = \langle I_j(\mathbf{r}_j, L) \rangle^2 \exp [H_{2j}(r_j, L)], \quad (19)$$

where

$$H_{2j}(r_j, L) = 8\pi^2 k_j^2 L \int_0^1 d\xi \int_0^\infty d\kappa \kappa \Phi_n(\kappa) \exp \left(-\frac{\Lambda_j L \kappa^2 \xi^2}{k_j} \right) \times \left\{ I_0(2\Lambda_j r_j \xi \kappa) - \cos \left[\frac{L \kappa^2 \xi (1 - \bar{\Theta}_j \xi)}{k_j} \right] \right\} \quad (20)$$

and $\bar{\Theta}_j = 1 - \Theta_j$. The cross-intensity term $\langle I_j(\mathbf{r}_j, L) I_m(\mathbf{r}_m, L) \rangle$ is given by (see Appendix A)

$$\begin{aligned} \langle I_j(\mathbf{r}_j, L) I_m(\mathbf{r}_m, L) \rangle &= \langle I_j(\mathbf{r}_j, L) \rangle \langle I_m(\mathbf{r}_m, L) \rangle \times \\ &\exp \{ E_{2jm}(\mathbf{r}_j, \mathbf{r}_m; k_j, k_m) + E_{2mj}(\mathbf{r}_m, \mathbf{r}_j; k_m, k_j) + \\ &2\text{Re} [E_{3jm}(\mathbf{r}_j, \mathbf{r}_m; k_j, k_m)] \}, \end{aligned} \quad (21)$$

where

$$E_{2jm}(\mathbf{r}_j, \mathbf{r}_m; k_j, k_m) = 4\pi^2 k_j k_m L \int_0^1 d\xi \int_0^\infty d\kappa \kappa \Phi_n(\kappa) J_0(\kappa |\gamma_j \mathbf{r}_j - \gamma_m^* \mathbf{r}_m|) \times \exp \left[-\frac{i}{2} \kappa^2 L \left(\frac{\gamma_j}{k_j} - \frac{\gamma_m^*}{k_m} \right) \xi \right], \quad (22)$$

$$E_{2mj}(\mathbf{r}_m, \mathbf{r}_j; k_m, k_j) = 4\pi^2 k_j k_m L \int_0^1 d\xi \int_0^\infty d\kappa \kappa \Phi_n(\kappa) J_0(\kappa |\gamma_m \mathbf{r}_m - \gamma_j^* \mathbf{r}_j|) \times \exp \left[-\frac{i}{2} \kappa^2 L \left(\frac{\gamma_m}{k_m} - \frac{\gamma_j^*}{k_j} \right) \xi \right] \quad (23)$$

and

$$E_{3jm}(\mathbf{r}_j, \mathbf{r}_m; k_j, k_m) = -4\pi^2 k_j k_m L \int_0^1 d\xi \int_0^\infty d\kappa \kappa \Phi_n(\kappa) J_0(\kappa |\gamma_j \mathbf{r}_j - \gamma_m \mathbf{r}_m|) \times \exp \left[-\frac{i}{2} \kappa^2 L \left(\frac{\gamma_j}{k_j} + \frac{\gamma_m}{k_m} \right) \xi \right]. \quad (24)$$

In Eqs. (22-24) $\gamma_j = 1 - (\bar{\Theta}_j + i\Lambda_j)\xi$.

SPECIFIC SETUPS, OPTIMAL CONFIGURATION AND REDUCTION OF THE TOTAL SCINTILLATION INDEX

We consider in detail a system with two lowest order Gaussian beams whose wavelengths are $\lambda_1 = 1.0 \times 10^{-6}\text{m}$ and $\lambda_2 = 1.01 \times 10^{-6}\text{m}$, and whose initial spot sizes are $W_{01} = W_{02} = 1.0\text{cm}$. The initial locations of the spot centers are $\mathbf{d}_1 = -d\hat{\mathbf{y}}/2$ and $\mathbf{d}_2 = d\hat{\mathbf{y}}/2$ so that the initial beam separation is d . We assume that the initial on-axis amplitudes are equal $A_{01} = A_{02}$ and that the beams are initially collimated so that $F_{01} = F_{02} = \infty$. We use the Von Kármán spectrum to describe the refractive index fluctuations

$$\Phi_n(\kappa) = 0.033 C_n^2 \frac{\exp(-\kappa^2/\kappa_{in}^2)}{(\kappa^2 + \kappa_{out}^2)^{11/6}} \quad (25)$$

where $\kappa_{in} = 5.92/l_0$, $\kappa_{out} = 1/L_0$, l_0 and L_0 are the turbulence inner and outer scales, respectively, and C_n^2 is the refractive index structure parameter. We choose $C_n^2 = 3.0 \times 10^{-15}\text{m}^{-2/3}$, corresponding to weak atmospheric turbulence conditions, and $l_0 = 1.0\text{mm}$, $L_0=1.0\text{m}$. We concentrate on the statistics at a propagation distance $L = 1\text{km}$, where the Rytov variance

$$\sigma_R^2 = 1.23 C_n^2 k^{7/6} L^{11/6} \quad (26)$$

is about 0.1 for both beams and one can indeed employ the Rytov perturbation method. The free space spot sizes of the beams at this distance are about 3.3cm each.

Using the above relations we first calculate the longitudinal component of the scintillation index as defined by Eq. (14). The longitudinal component is of special importance when the spot size is large compared with the radius of the receiver's collecting lens since in this case the average signal to noise ratio is predominantly determined by the on-axis values of $\langle I \rangle$ and $\langle I^2 \rangle$. The dependence of $\sigma_{I,l}^2$ on the initial separation between the two beams d for the aforementioned values of the parameters is plotted in Fig. 1 (solid line). It can be seen that the curve $\sigma_{I,l}^2(d; L)$ possesses a minimum at an intermediate value of d , $d_0 = 2.8\text{cm}$. Clearly this minimum corresponds to the optimal configuration of the two-beam system for the given physical parameters, where optimization is performed with respect to longitudinal scintillation. The figure also shows a comparison with the longitudinal scintillation of a single lowest order Gaussian beam with the same total power $P_0 = \pi A_0^2 W_0^2$ for the following two cases: (a) the single beam has the same initial spot size as that of each of the two beams (square); (b) the single beam has the same amplitude as that of each of the two beams (circle). One can see that the two-beam system gives a 53.4% reduction of the longitudinal scintillation in comparison with the single beam value in case (a) and a 56.9% reduction in comparison with the single beam result in case (b). The dashed line in Fig. 1 corresponds to the result obtained by using the Kolmogorov spectrum

$$\Phi_n(\kappa) = 0.033 C_n^2 \kappa^{-11/3}. \quad (27)$$

The dotted line corresponds to the approximate result obtained by using the Kolmogorov spectrum (27), assuming that for each beam $r_j < W_j$, and expanding up to the second order with respect to r_j/W_j . The comparison of these two results with the result based on the Von Kármán spectrum shows that for the parameters considered here the existence of the minimum of $\sigma_{I,l}^2(d; L)$ is not very sensitive to the details of the spectrum model. In addition, the minimum value of the longitudinal scintillation and the location of the minimum d_0 obtained by using the more realistic Von Kármán spectrum are slightly smaller than the values obtained by using the Kolmogorov spectrum.

In order to better understand the origin of the minimum of the longitudinal component of the scintillation index we further decompose $\sigma_{I,l}^2$ into a self-intensity contribution $\sigma_{I,l,s}^2$

and a cross-intensity contribution $\sigma_{I,l,c}^2$ in the following manner

$$\sigma_{I,l}^2 = \sigma_{I,l,s}^2 + \sigma_{I,l,c}^2 - 1, \quad (28)$$

where

$$\sigma_{I,l,s}^2(L) \equiv \frac{\langle I_1^2(d\hat{\mathbf{y}}/2, L) \rangle + \langle I_2^2(-d\hat{\mathbf{y}}/2, L) \rangle}{\langle I(\mathbf{0}, L) \rangle^2} \quad (29)$$

and

$$\sigma_{I,l,c}^2(L) \equiv \frac{2\langle I_1(d\hat{\mathbf{y}}/2, L)I_2(-d\hat{\mathbf{y}}/2, L) \rangle}{\langle I(\mathbf{0}, L) \rangle^2}. \quad (30)$$

The d dependence of the two components $\sigma_{I,l,s}^2$ and $\sigma_{I,l,c}^2$ is shown in Fig. 2 together with the d dependence of the total $\sigma_{I,l}^2$. As expected, the cross-intensity component $\sigma_{I,l,c}^2$ is a decreasing function of d . In contrast, $\sigma_{I,l,s}^2$ is increasing with increasing d due to the radial scintillation contribution of each beam. Thus, the existence of a minimum for $\sigma_{I,l}^2(d; L)$ is a direct consequence of this opposite behavior of the self- and cross-intensity contributions with increasing beam separation.

When the spot size is comparable with the radius of the receiver's collecting lens the radial component of the scintillation index becomes important and one should take into account both longitudinal and radial contributions. In Figure 3 we present the total scintillation index of the two-beam system for the optimal configuration, i.e. for $d = d_0 = 2.8\text{cm}$, in a $8\text{cm} \times 8\text{cm}$ domain centered about the z axis. The total scintillation index attains values in the range $0.011 < \sigma_I^2 < 0.474$. The minimum value of the scintillation is attained on the z axis since the two beams are already strongly overlapping at this distance, i.e., $d_0/2 < W_1, W_2$.

It is very instructive to analyze the reduction in the total scintillation index obtained by using the optimal two-beam system relative to a single lowest order Gaussian beam for cases (a) and (b) mentioned above. For this purpose we denote by $\sigma_{I,a}^2$ and $\sigma_{I,b}^2$ the total scintillation of a single beam in cases (a) and (b), respectively, and define the fractional reduction in the total scintillation relative to the single beam values in the two cases as

$$R_a(\mathbf{r}, L) = \frac{\sigma_{I,a}^2(\mathbf{r}, L) - \sigma_I^2(\mathbf{r}, L)}{\sigma_{I,a}^2(\mathbf{r}, L)} \quad (31)$$

and

$$R_b(\mathbf{r}, L) = \frac{\sigma_{I,b}^2(\mathbf{r}, L) - \sigma_I^2(\mathbf{r}, L)}{\sigma_{I,b}^2(\mathbf{r}, L)}. \quad (32)$$

Figure 4 shows $R_a(\mathbf{r}, L)$ in the $8\text{cm} \times 8\text{cm}$ domain. It can be seen that in case (a) the fractional reduction factor is in the range $0.124 < R_a < 0.639$ which means that the reduction is larger than 12.4% everywhere within the $8\text{cm} \times 8\text{cm}$ domain and can be as large as 63.9%. Similar calculation shows that the relative reduction in the total scintillation in case (b) is even larger. In both cases, the largest improvement is obtained along the y axis and in the corners of the domain. The smallest improvement is along the x axis, where the total intensity is initially small. This behavior suggests that in a 4-beam system further increase of the value of R can be obtained by locating the two additional beams along the x axis.

To get further insight into the results presented in Figs. 3 and 4 we decompose the total scintillation index into self- and cross-intensity contributions $\sigma_{I,s}^2$ and $\sigma_{I,c}^2$ in the following manner

$$\sigma_I^2(\mathbf{r}, L) = \sigma_{I,s}^2(\mathbf{r}, L) + \sigma_{I,c}^2(\mathbf{r}, L) - 1, \quad (33)$$

where

$$\sigma_{I,s}^2(\mathbf{r}, L) \equiv \frac{\langle I_1^2(\mathbf{r}_1, L) \rangle + \langle I_2^2(\mathbf{r}_2, L) \rangle}{\langle I(\mathbf{r}, L) \rangle^2} \quad (34)$$

and

$$\sigma_{I,c}^2(\mathbf{r}, L) \equiv \frac{2\langle I_1(\mathbf{r}_1, L)I_2(\mathbf{r}_2, L) \rangle}{\langle I(\mathbf{r}, L) \rangle^2}. \quad (35)$$

The self- and cross-intensity contributions to the total scintillation index for the optimal two-beam system are shown in Figures 5 and 6, respectively. The self-intensity contribution attains values in the range $0.523 < \sigma_{I,s}^2 < 1.354$ whereas the values of the cross-intensity contribution are in the range $0.052 < \sigma_{I,c}^2 < 0.582$. The largest values of $\sigma_{I,s}^2$ are attained in the corners of the $8\text{cm} \times 8\text{cm}$ domain, where the $\sigma_{I,c}^2$ contribution is negligible. It is also seen that the values of $\sigma_{I,s}^2$ are larger along the y axis and smaller along the x axis. This behavior is due to the contributions coming from the radial scintillation of each beam. The largest $\sigma_{I,c}^2$ values are attained on the x axis. These values are comparable to the values of $\sigma_{I,s}^2$ on the x axis which explains the relatively small values of R_a seen along the x axis in Fig. 4.

In analyzing the behavior of the radial scintillation we first note that unlike the situation in the single-beam case, in the two-beam case $\sigma_r^2(\mathbf{r}, L)$ is not radially symmetric. To enable comparison with the single-beam result we define the circularly averaged radial scintillation in the two-beam case σ_{rr}^2 as the average over angle θ of the radial scintillation index:

$\sigma_{rr}^2(r, L) \equiv \langle \sigma_r^2(\mathbf{r}, L) \rangle_\theta$. The r -dependence of σ_{rr}^2 for the optimal two-beam system is shown in Fig. 7. The figure also shows a comparison with the radial scintillation of a single lowest order Gaussian beam with the same total power and initial spot size. It can be seen that the value of the radial scintillation index for the optimal two-beam system at a given r is smaller by about 35%-40% than the corresponding value for the single beam. Therefore, optimizing the two-beam system with respect to the longitudinal scintillation also leads to a significant reduction in the radial scintillation.

CONCLUSIONS

We investigated the dynamics of two lowest order Gaussian laser beams with different wavelengths in weak atmospheric turbulence. Assuming a Von Kármán turbulence spectrum and slow detector response and using the Rytov approximation we calculated the longitudinal and radial components of the scintillation index for a typical free space laser communication setup. We found that the longitudinal scintillation possesses a minimum as a function of the initial beam separation. This minimum corresponds to the ideal configuration of the two beams, where optimization is performed with respect to the longitudinal scintillation index. The longitudinal scintillation for the optimal two-beam configuration is smaller by more than 50% compared with the value for a single lowest order Gaussian beam with the same total power. We introduced the self- and cross-intensity contributions to the longitudinal scintillation index and explained the existence of the minimum in terms of the opposite behavior of these contributions with increasing beam separation. Similar calculations of the longitudinal scintillation with the Kolmogorov spectrum show that the existence of the minimum is not very sensitive to the form of the turbulence spectrum.

In actual applications the radial component of the scintillation index might be as important as the longitudinal component. We therefore calculated the total scintillation index for the optimal two-beam configuration. We found that for the same typical setup considered above the values of the total scintillation are smaller by 12%-64% compared with the values of the total scintillation for a single beam with the same total power. Further analysis showed that the reduction of the scintillation obtained by using the optimal two-beam configuration was largest along the y axis, where the centers of the two beams are initially located, and smallest along the x axis, where the total intensity is initially small.

This behavior is attributed to the relatively large values of the cross-intensity contributions to the total scintillation along the x axis. It also suggests that in a four-beam configuration the system's performance can be further improved by locating the two additional beams along the x -axis. Finally, we showed that the circularly averaged radial scintillation index for the optimal two-beam configuration is smaller by 35%-40% compared with the radial scintillation for a single beam with the same total power.

The results presented in this paper open many promising pathways for future theoretical research. A natural extension of this study is to investigate a system with $N > 2$ Gaussian beams and to characterize the N -dependence of the scintillation reduction relative to the single beam case. Another possible direction is to study the dependence of the scintillation index in the multi-beam multi-wavelength case on the convergence/divergence of the beams, i.e., on the values of the phase front radii of curvature. Optimization with respect to the radial scintillation index at a given radius is yet another interesting problem. From the applications point of view it would be very interesting to evaluate the average signal to noise ratio and bit error rate of the multi-beam multi-wavelength system. This will require calculation of the optical field after the receiver's collecting lens as well as calculation of aperture averaging effects. Such calculations can be carried out in a straightforward manner by employing the ABCD ray matrix theory [3, 29].

Acknowledgments

We thank M. Kolesik, E. M. Wright, A. Marathay, J. T. Murray, P. Polynkin, M. Mansuripur and G. Gbur for very useful discussions. This research was sponsored by the Air Force Office for Scientific Research, Air Force Material Command, USAF, under grant AFOSR FA9550-04-1-0213.

DERIVATION OF EQS. (21)-(24)

In this appendix we derive Eqs. (21)-(24) for the cross-intensity term $\langle I_j(\mathbf{r}_j, L)I_m(\mathbf{r}_m, L) \rangle$. The derivation is based on the second order Rytov approximation and follows the outline of the calculation of $\langle I^2(\mathbf{r}, L) \rangle$ for a single lowest order Gaussian laser beam presented in chapters 5 and 6 of Ref. [3]. Within the framework of the Rytov approximation the optical

field of the j -th beam is given by Eq. (6). Therefore, the intensity of the j -th beam is

$$I_j(\mathbf{r}_j, L) = I_{0j}(\mathbf{r}_j, L) \exp [\psi_j(\mathbf{r}_j, L; k_j) + \psi_j^*(\mathbf{r}_j, L; k_j)], \quad (36)$$

where $I_{0j}(\mathbf{r}_j, L)$ is given by Eq. (17). It follows that

$$\langle I_j(\mathbf{r}_j, L) I_m(\mathbf{r}_m, L) \rangle = I_{0j}(\mathbf{r}_j, L) I_{0m}(\mathbf{r}_m, L) \exp \left[\Psi_{jm}^{(tot)}(\mathbf{r}, L) \right], \quad (37)$$

where

$$\Psi_{jm}^{(tot)}(\mathbf{r}, L) = \psi_j(\mathbf{r}_j, L; k_j) + \psi_j^*(\mathbf{r}_j, L; k_j) + \psi_m(\mathbf{r}_m, L; k_m) + \psi_m^*(\mathbf{r}_m, L; k_m). \quad (38)$$

Assuming that $\Psi_{ij}^{(tot)}$ is a Gaussian random variable [3] we can use the relation

$$\langle \exp \left[\Psi_{jm}^{(tot)}(\mathbf{r}, L) \right] \rangle = \exp \left\{ \langle \Psi_{jm}^{(tot)}(\mathbf{r}, L) \rangle + \left[\langle \Psi_{jm}^{(tot)2}(\mathbf{r}, L) \rangle - \langle \Psi_{jm}^{(tot)}(\mathbf{r}, L) \rangle^2 \right] \right\}. \quad (39)$$

We expand $\Psi_{jm}^{(tot)}(\mathbf{r}, L)$ up to the second order with respect to $n_1(\mathbf{r}, z)$

$$\begin{aligned} \Psi_{jm}^{(tot)}(\mathbf{r}, L) &\simeq \Psi_{jm1}^{(tot)}(\mathbf{r}, L) + \Psi_{jm2}^{(tot)}(\mathbf{r}, L) \simeq \\ &[\psi_{j1}(\mathbf{r}_j, L; k_j) + \psi_{j1}^*(\mathbf{r}_j, L; k_j) + \psi_{m1}(\mathbf{r}_m, L; k_m) + \psi_{m1}^*(\mathbf{r}_m, L; k_m)] + \\ &[\psi_{j2}(\mathbf{r}_j, L; k_j) + \psi_{j2}^*(\mathbf{r}_j, L; k_j) + \psi_{m2}(\mathbf{r}_m, L; k_m) + \psi_{m2}^*(\mathbf{r}_m, L; k_m)], \end{aligned} \quad (40)$$

where the subscripts 1 and 2 in ψ_1 and ψ_2 denote first and second order. Since $\langle n_1(\mathbf{r}, z) \rangle = 0$

$$\begin{aligned} \langle \Psi_{jm}^{(tot)}(\mathbf{r}, L) \rangle &\simeq \langle \Psi_{jm2}^{(tot)}(\mathbf{r}, L) \rangle = \langle \psi_{j2}(\mathbf{r}_j, L; k_j) \rangle + \langle \psi_{j2}^*(\mathbf{r}_j, L; k_j) \rangle + \\ &\langle \psi_{m2}(\mathbf{r}_m, L; k_m) \rangle + \langle \psi_{m2}^*(\mathbf{r}_m, L; k_m) \rangle \end{aligned} \quad (41)$$

and

$$\langle \Psi_{jm}^{(tot)}(\mathbf{r}, L) \rangle^2 \simeq \langle \Psi_{jm1}^{(tot)}(\mathbf{r}, L) \rangle^2 = 0. \quad (42)$$

In addition,

$$\begin{aligned} \langle \Psi_{jm}^{(tot)2}(\mathbf{r}, L) \rangle &\simeq \langle \Psi_{jm1}^{(tot)2}(\mathbf{r}, L) \rangle = \langle \psi_{j1}^2(\mathbf{r}_j, L; k_j) \rangle + \langle \psi_{j1}^{*2}(\mathbf{r}_j, L; k_j) \rangle + \\ &\langle \psi_{m1}^2(\mathbf{r}_m, L; k_m) \rangle + \langle \psi_{m1}^{*2}(\mathbf{r}_m, L; k_m) \rangle + E_{2jj}(\mathbf{r}_j, \mathbf{r}_j; k_j, k_j) + \\ &E_{2mm}(\mathbf{r}_m, \mathbf{r}_m; k_m, k_m) + E_{2jm}(\mathbf{r}_j, \mathbf{r}_m; k_j, k_m) + E_{2mj}(\mathbf{r}_m, \mathbf{r}_j; k_m, k_j) + \\ &2\text{Re} [E_{3jm}(\mathbf{r}_j, \mathbf{r}_m; k_j, k_m)], \end{aligned} \quad (43)$$

where

$$E_{2jm}(\mathbf{r}_j, \mathbf{r}_m; k_j, k_m) = \langle \psi_{j1}(\mathbf{r}_j, L; k_j) \psi_{m1}^*(\mathbf{r}_m, L; k_m) \rangle \quad (44)$$

and

$$E_{3jm}(\mathbf{r}_j, \mathbf{r}_m; k_j, k_m) = \langle \psi_{j1}(\mathbf{r}_j, L; k_j) \psi_{m1}(\mathbf{r}_m, L; k_m) \rangle. \quad (45)$$

Denoting

$$E_{1j}(\mathbf{r}_j; k_j) = \langle \psi_{j2}(\mathbf{r}_j, L; k_j) \rangle + \frac{1}{2} \langle \psi_{j1}^2(\mathbf{r}_j, L; k_j) \rangle \quad (46)$$

and using Eqs. (39)-(43) we obtain

$$\begin{aligned} \langle \exp \left[\Psi_{ij}^{(tot)}(\mathbf{r}, L) \right] \rangle &= \exp \{ 2E_{1j}(\mathbf{r}_j; k_j) + 2E_{1m}(\mathbf{r}_m; k_m) + \\ &E_{2jj}(\mathbf{r}_j, \mathbf{r}_j; k_j, k_j) + E_{2mm}(\mathbf{r}_m, \mathbf{r}_m; k_m, k_m) + E_{2jm}(\mathbf{r}_j, \mathbf{r}_m; k_j, k_m) + \\ &E_{2mj}(\mathbf{r}_m, \mathbf{r}_j; k_m, k_j) + 2\text{Re} [E_{3jm}(\mathbf{r}_j, \mathbf{r}_m; k_j, k_m)] \}. \end{aligned} \quad (47)$$

Noting that

$$\langle I_j(\mathbf{r}_j, L) \rangle = I_{0j}(\mathbf{r}_j, L) \exp [2E_{1j}(\mathbf{r}_j; k_j) + E_{2jj}(\mathbf{r}_j, \mathbf{r}_j; k_j, k_j)], \quad (48)$$

(see also Ref. [3] p. 130) we arrive at

$$\begin{aligned} \langle I_j(\mathbf{r}_j, L) I_m(\mathbf{r}_m, L) \rangle &= \langle I_j(\mathbf{r}_j, L) \rangle \langle I_m(\mathbf{r}_m, L) \rangle \times \\ &\exp \{ E_{2jm}(\mathbf{r}_j, \mathbf{r}_m; k_j, k_m) + E_{2mj}(\mathbf{r}_m, \mathbf{r}_j; k_m, k_j) + \\ &2\text{Re} [E_{3jm}(\mathbf{r}_j, \mathbf{r}_m; k_j, k_m)] \}, \end{aligned} \quad (49)$$

which is Eq. (21).

Next we derive Eq. (22) for $E_{2jm}(\mathbf{r}_j, \mathbf{r}_m; k_j, k_m)$. Within the framework of the Rytov perturbation method the first order term $\psi_{j1}(\mathbf{r}_j, L; k_j)$ is given by (see Ref. [3] p. 105)

$$\psi_{j1}(\mathbf{r}_j, L; k_j) = ik_j \int_0^L dz \iint d\nu(\mathbf{K}, z) \exp \left[i\gamma_j(z) \mathbf{K} \cdot \mathbf{r}_j - \frac{i\kappa^2 \gamma_j(z)(L-z)}{2k_j} \right], \quad (50)$$

where

$$\gamma_j(z) = \frac{1 + \alpha_j z}{1 + \alpha_j L} \quad (51)$$

and

$$\alpha_j = \frac{2}{k_j W_{0j}^2} + \frac{i}{F_{0j}}. \quad (52)$$

In Eq. (50) $\nu(\mathbf{K}, z)$ is the random amplitude of the refractive index fluctuations

$$n_1(\mathbf{r}, z) = \iint d\nu(\mathbf{K}, z) \exp(i\mathbf{K} \cdot \mathbf{r}), \quad (53)$$

$\mathbf{K} = (\kappa_x, \kappa_y)$ is the two-dimensional wave vector and $\kappa = (\kappa_x^2 + \kappa_y^2)^{1/2}$. Substituting Eq. (50) into Eq. (44) and using the correlation relation

$$\langle \nu(\mathbf{K}, z) \nu^*(\mathbf{K}', z') \rangle = F_n(\mathbf{K}, |z - z'|) \delta(\mathbf{K} - \mathbf{K}') d^2\mathbf{K} d^2\mathbf{K}' \quad (54)$$

where $\delta(\mathbf{K})$ stands for the Dirac delta function and $F_n(\mathbf{K}, |z - z'|)$ is the two-dimensional spectral density of the refractive index fluctuations we obtain

$$E_{2jm}(\mathbf{r}_j, \mathbf{r}_m; k_j, k_m) = k_j k_m \int_0^L dz \int_0^L dz' \iint d^2\mathbf{K} F_n(\mathbf{K}, |z - z'|) \times \exp \left\{ i\mathbf{K} \cdot [\gamma_j(z)\mathbf{r}_j - \gamma_m^*(z')\mathbf{r}_m] - \frac{i\kappa^2}{2} \left[\frac{\gamma_j(z)(L - z)}{k_j} - \frac{\gamma_m^*(z')(L - z')}{k_m} \right] \right\}. \quad (55)$$

We now change variables from z and z' to $\mu = z - z'$ and $\eta = (z + z')/2$. In addition, we use the fact that $F_n(\mathbf{K}, |\mu|)$ is centered about $\mu = 0$ to extend the integration over μ to $\pm\infty$ and to take $z = z' = \eta$. This calculation yields

$$E_{2jm}(\mathbf{r}_j, \mathbf{r}_m; k_j, k_m) = k_j k_m \int_0^L d\eta \iint d^2\mathbf{K} \int_{-\infty}^{\infty} d\mu F_n(\mathbf{K}, |\mu|) \times \exp \left\{ i\mathbf{K} \cdot [\gamma_j(\eta)\mathbf{r}_j - \gamma_m^*(\eta)\mathbf{r}_m] - \frac{i\kappa^2}{2} \left[\frac{\gamma_j(\eta)}{k_j} - \frac{\gamma_m^*(\eta)}{k_m} \right] (L - \eta) \right\}. \quad (56)$$

The two-dimensional spectral density is related to the power spectral density $\Phi_n(\mathbf{K})$ via

$$\Phi_n(\mathbf{K}) = \frac{1}{2\pi} \int_{-\infty}^{\infty} d\mu F_n(\mathbf{K}, |\mu|). \quad (57)$$

We assume that the turbulence is statistically homogeneous and isotropic so that $\Phi_n(\mathbf{K}) = \Phi_n(\kappa)$. Substituting Eq. (57) into Eq. (56) and performing integration over the angular coordinate in \mathbf{K} -space we obtain

$$E_{2jm}(\mathbf{r}_j, \mathbf{r}_m; k_j, k_m) = 4\pi^2 k_j k_m \int_0^L d\eta \int_0^{\infty} d\kappa \kappa \Phi_n(\kappa) J_0(\kappa |\gamma_j \mathbf{r}_j - \gamma_m^* \mathbf{r}_m|) \times \exp \left\{ -\frac{i\kappa^2}{2} \left[\frac{\gamma_j(\eta)}{k_j} - \frac{\gamma_m^*(\eta)}{k_m} \right] (L - \eta) \right\}. \quad (58)$$

Changing variables from η to the normalized distance $\xi = 1 - \eta/L$ we arrive at

$$E_{2jm}(\mathbf{r}_j, \mathbf{r}_m; k_j, k_m) = 4\pi^2 k_j k_m \int_0^1 d\xi \int_0^\infty d\kappa \kappa \Phi_n(\kappa) J_0(\kappa |\gamma_j \mathbf{r}_j - \gamma_m^* \mathbf{r}_m|) \times \exp \left[-\frac{i}{2} \kappa^2 L \left(\frac{\gamma_j}{k_j} - \frac{\gamma_m^*}{k_m} \right) \xi \right], \quad (59)$$

which is Eq. (22). Equation (23) for $E_{2mj}(\mathbf{r}_m, \mathbf{r}_j; k_m, k_j)$ and Eq. (24) for $E_{3jm}(\mathbf{r}_j, \mathbf{r}_m; k_j, k_m)$ are obtained in a similar manner.

* Electronic address: avner@acms.arizona.edu

- [1] A. Ishimaru, *Laser Wave Propagation and Scattering in Random Media, Vol. 2*, (Academic, New York, 1978).
- [2] R. L. Fante, "Wave propagation in random media: a systems approach," in *Progress in Optics, Vol. XXII*, E. Wolf, ed. (Elsevier, New York, 1985).
- [3] L. C. Andrews and R. L. Phillips, *Laser Beam Propagation through Random Media* (SPIE Press, Bellingham, Washington, 1998).
- [4] M. S. Belenkii, A. I. Kon, and V. L. Mironov, "Turbulence distortions of the spatial coherence of a laser beam," *Sov. J. Quantum Electron.* **7**, 287-290 (1977).
- [5] S. C. H. Wang and M. A. Plonus, "Optical beam propagation for a partially coherent source in the turbulent atmosphere," *J. Opt. Soc. Am.* **69**, 1297-1304 (1979).
- [6] M. S. Belenkii and V. L. Mironov, "Coherence of the field of a laser beam in a turbulent atmosphere," *Sov. J. Quantum Electron.* **10**, 595-597 (1980).
- [7] V. A. Banakh, V. M. Buldakov, and V.L. Mironov, "Intensity fluctuations of a partially coherent light beam in a turbulent atmosphere," *Opt. Spektrosk.* **54**, 1054-1059 (1983).
- [8] V. A. Banakh and V. M. Buldakov, "Effect of the initial degree of spatial coherence of a light beam on intensity fluctuations in a turbulent atmosphere," *Opt. Spektrosk.* **55**, 757-762 (1983).
- [9] J. Wu, "Propagation of a Gaussian-Schell beam through turbulent media," *J. Mod. Opt.* **37**, 671-684 (1990).
- [10] J. Wu and A. D. Boardman, "Coherence length of a Gaussian Schell-model beam and atmospheric turbulence," *J. Mod. Opt.* **38**, 1355-1363 (1991).

- [11] G. Gbur and E. Wolf, "Spreading of partially coherent beams in random media," *J. Opt. Soc. Am. A* **19**, 1592-1598 (2002).
- [12] A. Dogariu and S. Amarande, "Propagation of partially coherent beams: turbulence-induced degradation," *Opt. Lett.* **28**, 10-12, (2003).
- [13] T. Shirai, A. Dogariu, and E. Wolf, "Mode analysis of spreading of partially coherent beams propagating through atmospheric turbulence," *J. Opt. Soc. Am. A* **20**, 1094-1102 (2003).
- [14] M. Salem, T. Shirai, A. Dogariu, and E. Wolf, "Long-distance propagation of partially coherent beams through atmospheric turbulence," *Opt. Commun.* **216**, 261-265 (2003).
- [15] X. Ji and B. Lü, "Turbulence-induced quality degradation of partially coherent beams," *Opt. Commun.* **251**, 231-236 (2005).
- [16] O. Korotkova, L. C. Andrews, and R. L. Phillips, "Model for a partially coherent Gaussian beam in atmospheric turbulence with application in lasercom," *Opt. Eng.* **43**, 330-341 (2004).
- [17] J. C. Ricklin and F. M. Davidson, "Atmospheric turbulence effects on a partially coherent Gaussian beam: implications for free-space laser communication," *J. Opt. Soc. Am. A* **19**, 1794-1802 (2002).
- [18] J. C. Ricklin and F. M. Davidson, "Atmospheric optical communication with a Gaussian Schell beam," *J. Opt. Soc. Am. A* **20**, 856-866 (2003).
- [19] T. J. Schulz, "Optimal beams for propagation through random media", *Opt. Lett.* **30**, 1093-1095 (2005).
- [20] L. Fan, M. Fallahi, J. T. Murray, R. Bedford, Y. Kaneda, A. R. Zakharian, J. Hader, J. V. Moloney, W. Stolz, and S. W. Koch, "Tunable high-power high-brightness linearly polarized vertical-external-cavity surface emitting lasers," *App. Phys. Lett.* **88**, 0211051 - 0211053 (2006).
- [21] Coherent Inc., Santa Clara, California (personal communication, 2005).
- [22] J. L. A. Chilla, S. D. Butterworth, A. Zeitschel, J. P. Charles, A. L. Caprara, M. K. Reed, and L. Spinelli, "High-power optically pumped semiconductor lasers," in *Nanobiophotonics and Biomedical Applications*, A. N. Cartwright, ed., *Proc. SPIE* **5332**, 143-150 (2004).
- [23] R. L. Fante, "Effect of source bandwidth and receiver response time on the scintillation index in random media," *Radio Sci.* **12**, 223-229 (1977).
- [24] R. L. Fante, "The effect of source temporal coherence on light scintillation in weak turbulence," *J. Opt. Soc. Am.* **69**, 71-73 (1979).

- [25] R. L. Fante, “Intensity fluctuations of an optical wave in a turbulent medium, effect of source coherence,” *Opt. Acta* **28**, 1203-1207 (1981).
- [26] Y. Baykal, M. A. Plonus, and S. J. Wang, “The scintillations for weak atmospheric turbulence using a partially coherent source,” *Radio Sci.* **18**, 551-556 (1983).
- [27] K. Kiasaleh, “Scintillation index of a multiwavelength beam in turbulent atmosphere”, *J. Opt. Soc. Am. B* **21**, 1452-1454 (2004).
- [28] K. Kiasaleh, “Impact of turbulence on multi-wavelength coherent optical communications,” in *Free-Space Laser Communications V*, D. G. Voelz and J. C. Ricklin, eds., *Proc. SPIE* **5892**, 58920R1-58920R11 (2005).
- [29] L. C. Andrews, R. L. Phillips, and C. Y. Hopen, *Laser Beam Scintillation with Applications* (SPIE Press, Bellingham, Washington, 2001).
- [30] M. Abramowitz and I. A. Stegun, *Handbook of Mathematical Functions*, (National Bureau of Standards, Washington, D.C., 1968).

LIST OF FIGURE CAPTIONS

Fig. 1. Longitudinal component of the scintillation index $\sigma_{I,l}^2$ as a function of the initial beam separation d . The solid line is the result obtained by using the the Von Kármán spectrum. The dashed line is the result obtained by using the Kolmogorov spectrum and the dotted line corresponds to the result obtained by using the Kolmogorov spectrum and assuming that $r_j/W_j \ll 1$. The square/circle stand for the longitudinal scintillation of a single beam with the same total power and the same initial spot size/amplitude, respectively.

Fig. 2. Self- and cross-intensity contributions to the longitudinal scintillation index $\sigma_{I,l,s}^2$ and $\sigma_{I,l,c}^2$, respectively, vs beam separation d . The dashed line represents $\sigma_{I,l,s}^2(d; L)$ and the dotted line stands for $\sigma_{I,l,c}^2(d; L)$. The solid line corresponds to $\sigma_{I,l}^2(d; L) + 1/2$.

Fig. 3. Total scintillation index $\sigma_I^2(\mathbf{r}, L)$ for the two-beam system with the optimal configuration $d_0 = 2.8\text{cm}$ at a propagation distance $L = 1\text{km}$. The figure shows a $8\text{cm} \times 8\text{cm}$ domain centered about the z axis.

Fig. 4. Fractional reduction of the total scintillation index $R_a(\mathbf{r}, L)$ obtained by using the optimal two-beam system relative to a single Gaussian beam with the same total intensity and initial spot size.

Fig. 5. Self-intensity contribution to the total scintillation index $\sigma_{I,s}^2(\mathbf{r}, L)$ for the optimal two-beam system.

Fig. 6. Cross-intensity contribution to the total scintillation index $\sigma_{I,c}^2(\mathbf{r}, L)$ for the optimal two-beam system.

Fig. 7. Circularly averaged radial scintillation index for the optimal two-beam system σ_{rr}^2 as a function of radius r (circles). The squares correspond to the result obtained for a single beam with the same power and initial spot size.

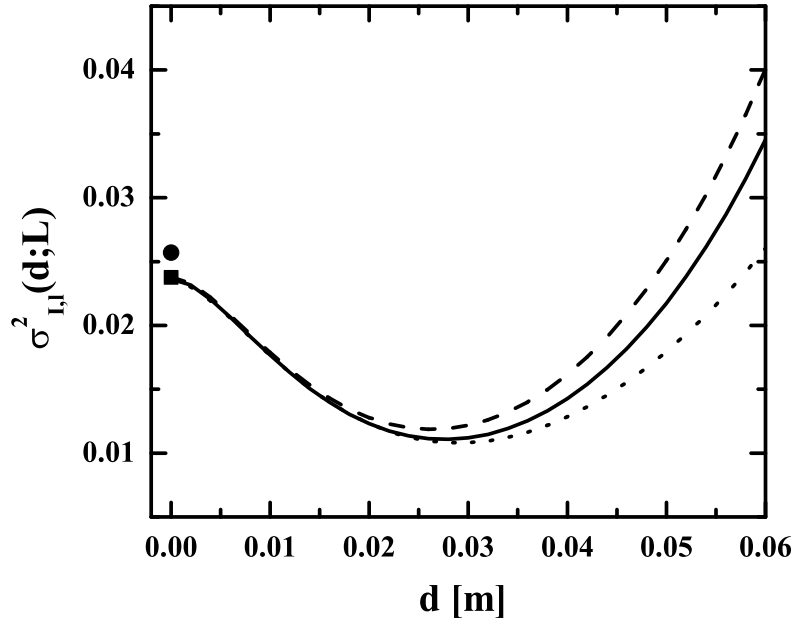


FIG. 1: Longitudinal component of the scintillation index $\sigma_{I,l}^2$ as a function of the initial beam separation d . The solid line is the result obtained by using the the Von Kármán spectrum. The dashed line is the result obtained by using the Kolmogorov spectrum and the dotted line corresponds to the result obtained by using the Kolmogorov spectrum and assuming that $r_j/W_j \ll 1$. The square/circle stand for the longitudinal scintillation of a single beam with the same total power and the same initial spot size/amplitude, respectively.

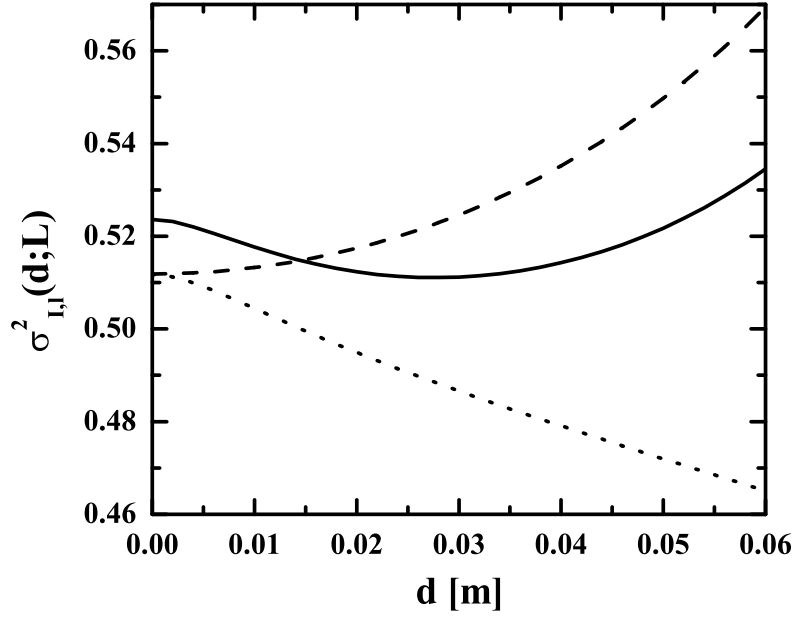


FIG. 2: Self- and cross-intensity contributions to the longitudinal scintillation index $\sigma^2_{I,l,s}$ and $\sigma^2_{I,l,c}$, respectively, vs beam separation d . The dashed line represents $\sigma^2_{I,l,s}(d;L)$ and the dotted line stands for $\sigma^2_{I,l,c}(d;L)$. The solid line corresponds to $\sigma^2_{I,l}(d;L) + 1/2$.

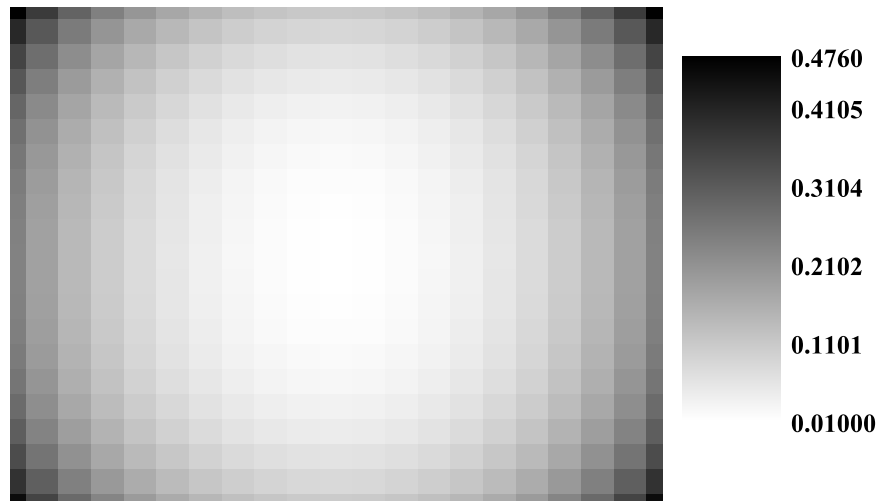


FIG. 3: Total scintillation index $\sigma_I^2(\mathbf{r}, L)$ for the two-beam system with the optimal configuration $d_0 = 2.8\text{cm}$ at a propagation distance $L = 1\text{km}$. The figure shows a $8\text{cm} \times 8\text{cm}$ domain centered about the z axis.

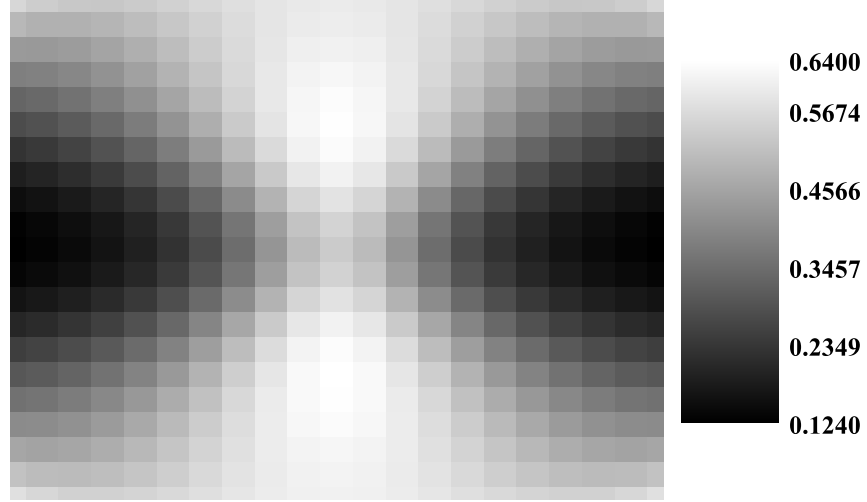


FIG. 4: Fractional reduction of the total scintillation index $R_a(\mathbf{r}, L)$ obtained by using the optimal two-beam system relative to a single Gaussian beam with the same total intensity and initial spot size.

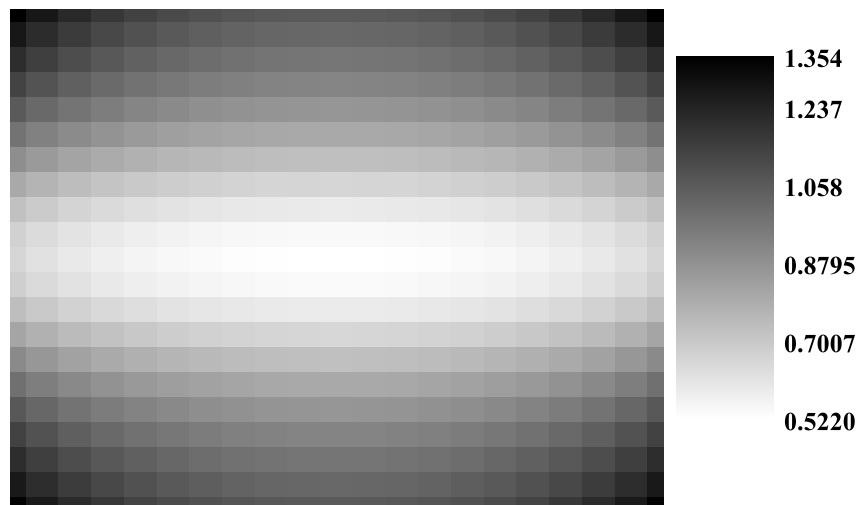


FIG. 5: Self-intensity contribution to the total scintillation index $\sigma_{I,s}^2(\mathbf{r}, L)$ for the optimal two-beam system.

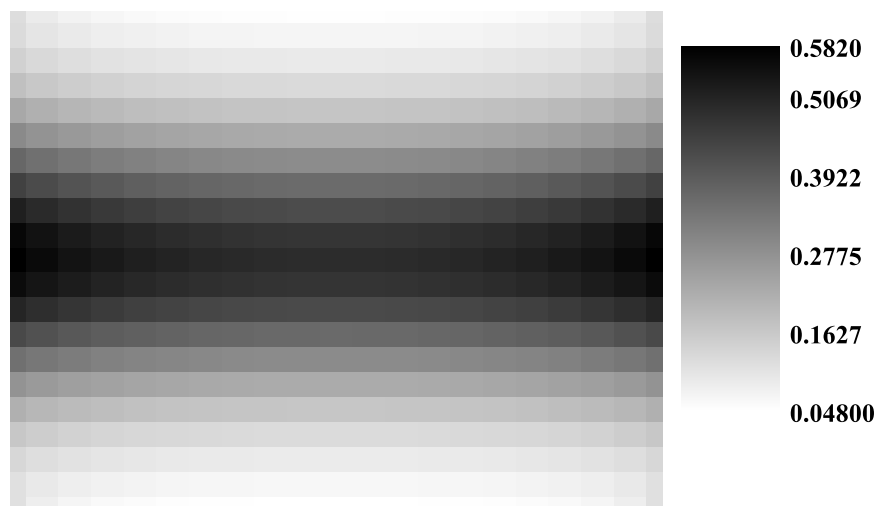


FIG. 6: Cross-intensity contribution to the total scintillation index $\sigma_{I,c}^2(\mathbf{r}, L)$ for the optimal two-beam system.

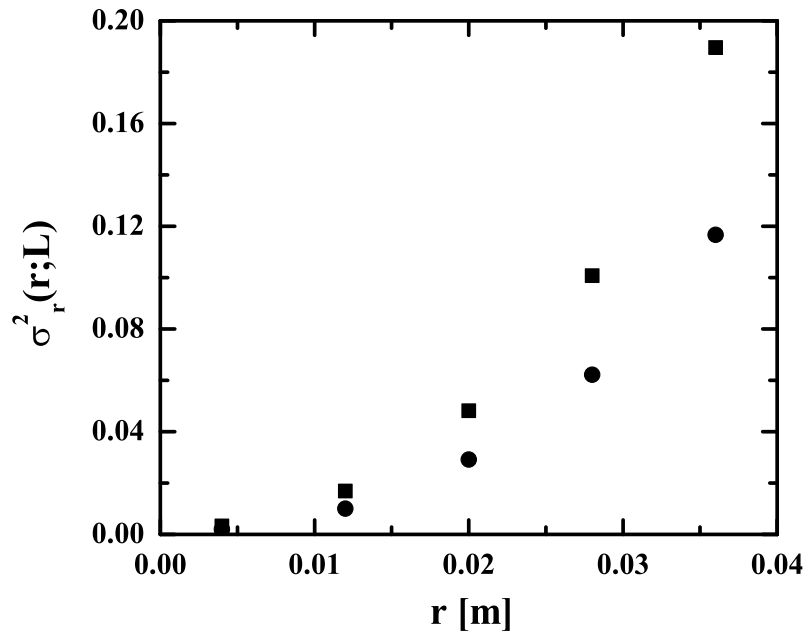


FIG. 7: Circularly averaged radial scintillation index for the optimal two-beam system σ_{rr}^2 as a function of radius r (circles). The squares correspond to the result obtained for a single beam with the same power and initial spot size.